# REPORT DOCUMENTATION PAGE

*Form Approved*
*OMB No. 0704-0188*



**PLEASE DO NOT RETURN YOUR FORM TO THE ABOVE ORGANIZATION.**

| 1. REPORT DATE *(DD-MM-YYYY)* | 2. REPORT TYPE | 3. DATES COVERED *(From - To)* |
|---|---|---|
| 11-14-2008 | Final Performance Report | 08-15-2007 - 08-14-2008 |

**4. TITLE AND SUBTITLE**

Optimizing Grain Boundary Complexions to Produce Dense Pressure-less Sintered Boron Carbide (B4C)

**5a. CONTRACT NUMBER**

**5b. GRANT NUMBER**
FA9550-07-1-0564

**5c. PROGRAM ELEMENT NUMBER**

**6. AUTHOR(S)**

Harmer, Martin P.
Dillon, Shen J.

**5d. PROJECT NUMBER**

**5e. TASK NUMBER**

**5f. WORK UNIT NUMBER**

**7. PERFORMING ORGANIZATION NAME(S) AND ADDRESS(ES)**

Lehigh University
Center for Advanced Materials and Nanotechnology
5 East Packer Avenue
Bethlehem, PA 18015

**8. PERFORMING ORGANIZATION REPORT NUMBER**

**9. SPONSORING/MONITORING AGENCY NAME(S) AND ADDRESS(ES)**

Dr. Joan Fuller/NA
Air Force Office of Scientific Research
875 North Randolph Street
Suite 325, Rm 3112
Arlington, VA 22203

**10. SPONSOR/MONITOR'S ACRONYM(S)**
AFOSR

**11. SPONSOR/MONITOR'S REPORT NUMBER(S)**
AFRL-SR-AR-TR-08-0531

**12. DISTRIBUTION/AVAILABILITY STATEMENT**

Approved for public release; distribution unlimited.



**13. SUPPLEMENTARY NOTES**

**14. ABSTRACT**

The goal of this seedling grant was to explore the possible existence and role of grain boundary complexions in the sintering of boron carbide by two means. First, we have developed a novel processing strategy, which exploits the use of a chemical (dopant) gradient in order to facilitate the ease of identification and characterization of grain boundary complexions. Second, we have characterized commercially prepared samples in which different dopants led to significant differences in grain growth behavior (abnormal versus abnormal). The results of this study determined that sintering and grain growth in boron carbide is highly sensitive to dopant chemistry and amount. The chemical gradient model experiment revealed that yttria can readily activate complexion transitions in boron carbide. Alumina promotes abnormal grain growth in boron carbide by activating a grain boundary complexion transition from type I (sub monolayer adsorption) to type III (multilayer adsorption). The use of multiple dopants is effective in stabilizing grain boundary complexion type I in boron carbide and in preventing abnormal grain growth. Further work on the identification and control of grain boundary complexions in boron carbide is highly recommended.

**15. SUBJECT TERMS**

complexions, grain boundaries, ceramic armor, boron carbide

| 16. SECURITY CLASSIFICATION OF: | | | 17. LIMITATION OF ABSTRACT | 18. NUMBER OF PAGES | 19a. NAME OF RESPONSIBLE PERSON |
|---|---|---|---|---|---|
| a. REPORT | b. ABSTRACT | c. THIS PAGE | | | Martin P. Harmer |
| Unclassified | Unclassified | Unclassified | Unlimited | 15 | 19b. TELEPHONE NUMBER *(Include area code)* 610-758-4227 |

## Introduction

Boron carbide ($B_4C$) is the current material of choice for ceramic armor because of its low density (2.52 g/cc) and extremely high hardness (3770 kg/mm$^2$). Such application demands fully densified monolithic structures of boron carbide. Sintering of boron carbide to near theoretical densities has been proved to be the most significant challenge in this regard. Often specific additives such as carbon, $Al_2O_3$ and $TiB_2$ and/or hot pressing have been employed to achieve near theoretical density. However, the presence of additives can stimulate abnormal grain growth and the formation of non uniform microstructures, which reduces its mechanical strength. Furthermore, hot pressing prohibits the manufacturing of complex shapes required for ceramic armors. Therefore, the ideal solution would be to pressure-less sinter boron carbide to high density with controlled grain size and uniform grain size distribution. Unfortunately, this has been difficult to do in the past because of the lack of fundamental understanding of how additives work. The recent discovery of interface "complexions" has opened up a totally new avenue for understanding and predicting the effect of additives on microstructure development, which is one of the main goals of the current project.

In both oxide and non-oxide ceramics, good sinterability is often associated with the presence of intergranular films that promote densification by increasing the grain boundary diffusivity. The use of different dopants including $Yb_2O_3$, $Al_2O_3$, MgO, CaO etc to achieve near theoretical density in silicon nitride and silicon carbide by the formation of intergranular films (IGF's) is well documented.[1-25] However IGF's are just one type of "complexion". Recent work by the present authors on alumina has verified the existence of as many as six different types of interface complexions in materials.[26-28] They are shown schematically in Figure 1. Complexions I, II and III contain no intergranular film, whereas the other three do. Complexion I represents sub-monolayer segregation of dopants or impurities in the grain boundary core that results in solute drag. Type II complexion is the clean grain boundary of intrinsic grain growth associated with undoped alumina. Complexion III shows bi-layer segregation of dopants at the grain boundaries. Multi-layer segregation of dopants to the aluminum sites at the grain boundaries results in the formation of ~0.6 nm intergaranular film in complexion IV. Complexion V is characterized by a thin intergranular film of thickness of the order of 1 – 2 nm. Complexion VI exhibits a wetting grain boundary film of thickness greater than 4 nm.

Each of these complexions has a distinct boundary transport rate as shown in Figure 2. The grain boundary mobility increases with increasing grain boundary disorder, grain boundary width or grain boundary free volume. The grain boundary transport kinetics can vary by up to 4 orders of magnitude depending on the type of complexion. For example, grain boundaries with type V complexion exhibit grain boundary mobilities 50 times faster than those for normal grain growth in undoped alumina. Similarly, over two orders of magnitude larger grain boundary mobility has been observed in type VI grain boundaries as compared to normal grain growth in undoped alumina. Different grain boundary complexions can be induced in alumina by using different dopants. Transition of grain boundary complexion is also a function of temperature.

Although present as a very small volume fraction, the grain boundary phases (complexions) can determine the macroscopic properties. If more than one grain boundary complexion coexists in a microstructure, abnormal grain growth will occur. High strength materials can be obtained by

stabilizing one single complexion type in a microstructure, thereby preventing abnormal grain growth. The authors have demonstrated that this is the mechanism by which magnesia suppresses abnormal grain growth in alumina. Type I complexion is also associated with reduction in transport properties such as creep and oxidation. Type V complexions are known to weaken the grain boundary significantly, which can be exploited in increasing the fracture toughness in the ceramics by crack deflection along the boundaries and grain bridging. These few examples demonstrate the need of systematic study of these complexions in designing materials with properties tailor-made for specific applications.

As mentioned earlier, the intergranular films that have been observed in silicon nitride and silicon carbide are only one the possibe one of the different grain boundary complexions that might be present a material such s boron carbide. There have been no previous studies of complexions in boron carbide. A systematic study of the grain boundaries and complexion types in these materials can provide a predictive tool for achieving better sinterability in these materials. In boron carbide different additives including SiC,[29] $Al_2O_3$,[30] $TiB_2$,[31] $AlF_3$,[32] $W_2B_5$[33] have been reported to enhance densification. However the most well known additive for achieving highly dense boron carbide by pressureless sintering is carbon. Carbon added to boron carbide in the form of phenolic resin facilitated densification up to 98% of theoretical density at 2150° C. it has been argued that the presence of boron oxide ($B_2O_3$) in the starting boron carbide powders promotes surface diffusion resulting in coarsening of the boron carbide compacts and carbon addition eliminates boron oxide by removing oxygen incorporated in boron oxide. However the actual mechanism of enhanced surface diffusion because of the presence of the boron oxide and the exact reactions between boron oxide and carbon are debatable. In general, a fundamental understanding of the effect of additives on grain boundary structure and transport is lacking, especially given the new discovery of grain boundary complexions. It is speculated by the authors of this work that additives are playing a major role in activating grain boundary complexion transitions in boron carbide, thus influencing the sinterability in significant ways that were not previously appreciated. To the best of our knowledge there has been very little previous work on the characterization of the grain boundaries in boron carbide by high resolution electron microscopy, which is an essential requirement for understanding the sintering behavior by controlling the grain boundary complexions.

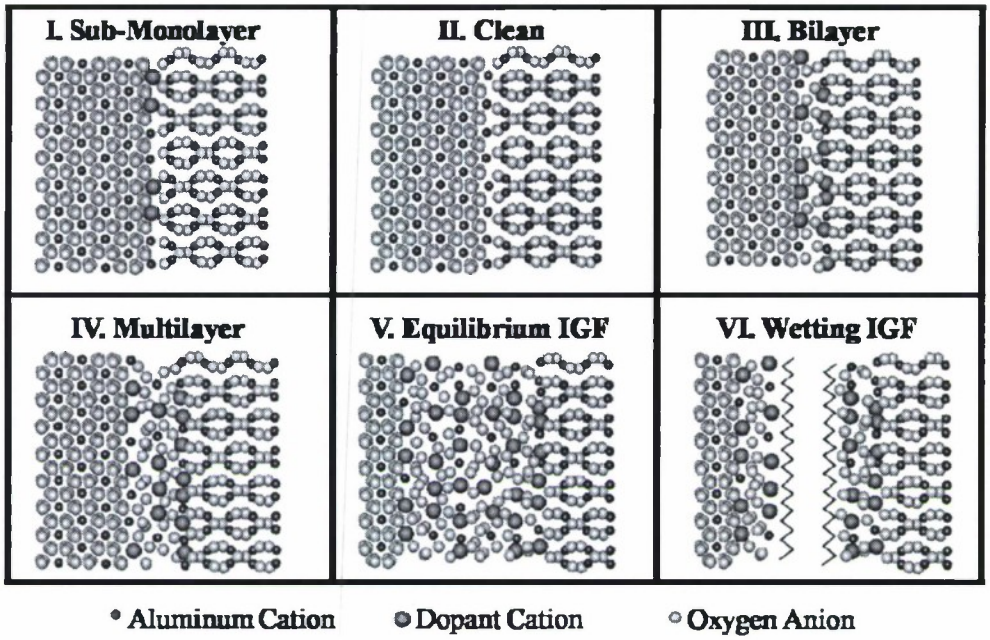


Figure 1. Schematic of Complexion types.

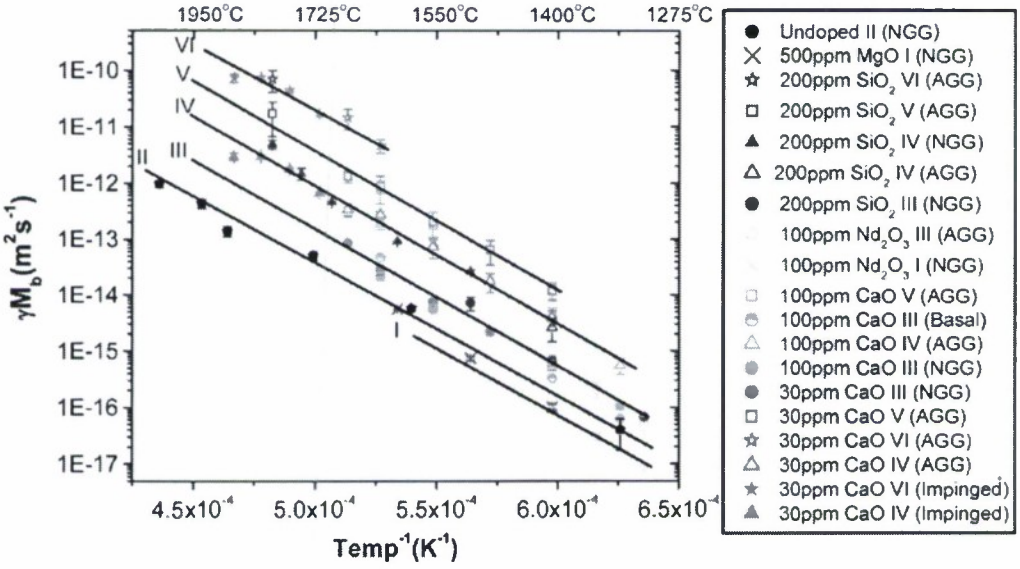


Figure 2. The grain boundary mobility versus inverse temperature for undoped and variously doped aluminas classified into six distinct categories according to the complexion type.

## Objectives of the Seedling Grant

The goal of this seedling grant was to explore the possible existence and role of grain boundary complexions in the sintering of boron carbide by two means. First, we have developed a novel processing strategy, which exploits the use of a chemical (dopant) gradient in order to facilitate the ease of identification and characterization of grain boundary complexions. Second, we have characterized commercially prepared samples in which different dopants led to significant differences in grain growth behavior (abnormal versus abnormal). Given that boron carbide is an extremely mechanically hard material it was also anticipated that a significant effort would be needed to develop the critically important procedures for preparing high quality specimens for transmission electron microscopy characterization.

## Results and Discussion

To investigate the grain boundary complexions in boron carbide two sets of sample were used as shown in table I. The first set of samples was prepared at Lehigh University. The samples were prepared using H.C.Starck HD20 boron carbide powder. The properties of the powder are shown in table II. Undoped boron carbide samples were prepared as a control set. Ytrria doped boron carbide was prepared to investigate the effect of a well known sintering aid in boron carbide. All the samples were hot pressed in vacuum at 1750°C for 1 hour under a pressure of 40 MPa. The hot pressing was followed by heat treatment at 1950°C for different periods of time. The samples were cut, polished and thermally etched at 1700°C for 30 minutes in vacuum for better visibility of the grain boundaries. Yttria was added to the boron carbide in solution form (yttrium nitrate dissolved in acetone) to ensure homogeneous mixture of yttrium oxide and boron carbide. The mixture was milled and pre-treated to decompose yttrium nitrate to yttria. The second set of samples was provided by PPG industries. The first sample had 05 wt% alumina dopant, whereas the second set contained multiple dopants including oxides of aluminum, magnesium, and silicon.

Table I. Samples Investigated in this Research

| | |
|---|---|
| Lehigh University Samples | Undoped Boron Carbide<br>1 wt. % Yttria doped Boron Carbide<br>Yttria-Boron Carbide Sandwich Structures |
| PPG samples | PPG#161 R3 (Al 0.5 wt.%)<br>PPG 166 (Multi dopant, Al, Mg, Si, ---) |

Table II. Properties of HD20 Boron Carbide Powder[34]

| | |
|---|---|
| Boron:Carbon Ratio | 3.7 – 3.9 |
| Average Particle Size / Laser Diffraction $d_{50}$ µm | 0.5 |
| Specific Surface Area (BET) $m^2/g$ | 22.0 – 27.0 |

In order to investigate the effect of yttria a novel experiment was designed involving a sandwich structure. Figure 3 shows a schematic of the sandwich structure. It consists of a thin layer of powder containing equal amounts of boron carbide and yttria sandwiched between two thick layers of boron

carbide. The idea behind this concept was that during the heat-treatment of the sample yttria will diffuse through the boron carbide layers creating a concentration gradient of yttria through the boron carbide. One might expect to see a transition in complexion type from high to low with increasing distance from the interface, which will manifest itself in changes in corresponding grain growth rates within the gradient region. Thus, from a single experiment, the effect of a dopant (in this particular case yttria) on compexion transitions in boron carbide can be assessed. The sample was hot-pressed and heat-treated following the same schedule as mentioned before. The duration of heat treatment was 15 hours.

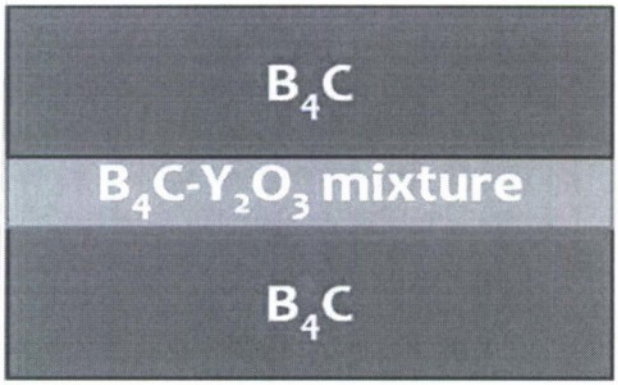


Figure 3. Schematic of boron carbide yttria sandwich structure.

A mixture of yttria and boron carbide was found to be necessary for good adhesion between the yttria and boron carbide layers. It was observed in the early experiments that macroscopic cracks were developed between the yttria and boron carbide layers when pure yttria was used as the middle layer and the entire sandwich structure fall apart. A 1:1 mixture of yttria and boron carbide provided optimum results; there were no cracks between the layers and yttrium was well distributed within the boron carbide layers.

**Boron carbide at Lehigh University**

The undoped boron carbide sample had a uniform grain size distribution with average grain size of ~20 μm as observed in the SEM (figure 4). Both inter- and intra-granular pores were present in the sample. Also, there was no significant change in grain size when the heat treatment time was increased to 18 hours from 5 hours. In comparison, an average grain size of ~50 μm was observed for the 1 wt. % yttria doped sample (Figure 5). It can be clearly seen that yttria is segregated predominantly at the triple junctions and in some occasions along the grain boundaries. The sharp contrast in the backscattered electron image is primarily due to the difference in mass between yttrium and boron/carbon atoms. Small pores were included in the grains. The large pores are attributed to pull-out from the triple junctions as evident from the secondary electron image. This indicates a very weak interface between yttria and boron carbide.

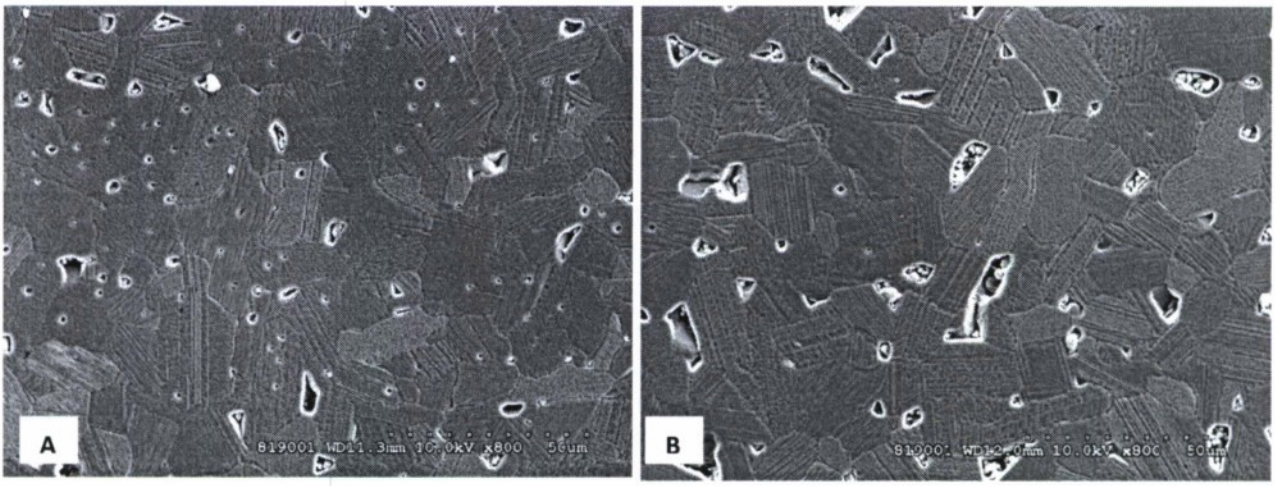


Figure 4. SEM images of undoped boron carbide powder heat treated at 1900°C for different time periods; (A) 5 hours, (B) 18 hours.

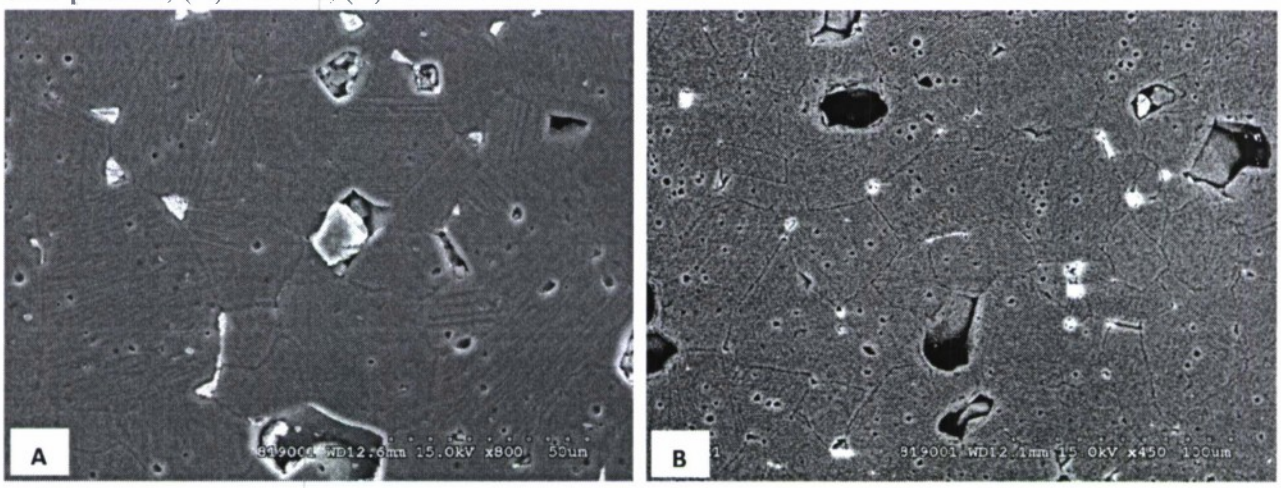


Figure 5. SEM images of 1 wt.% yttria doped boron carbide powder heat treated at 1900°C for 18 hours; (A) Secondary electron image from a ET detector, (B) Backscattered electron image.

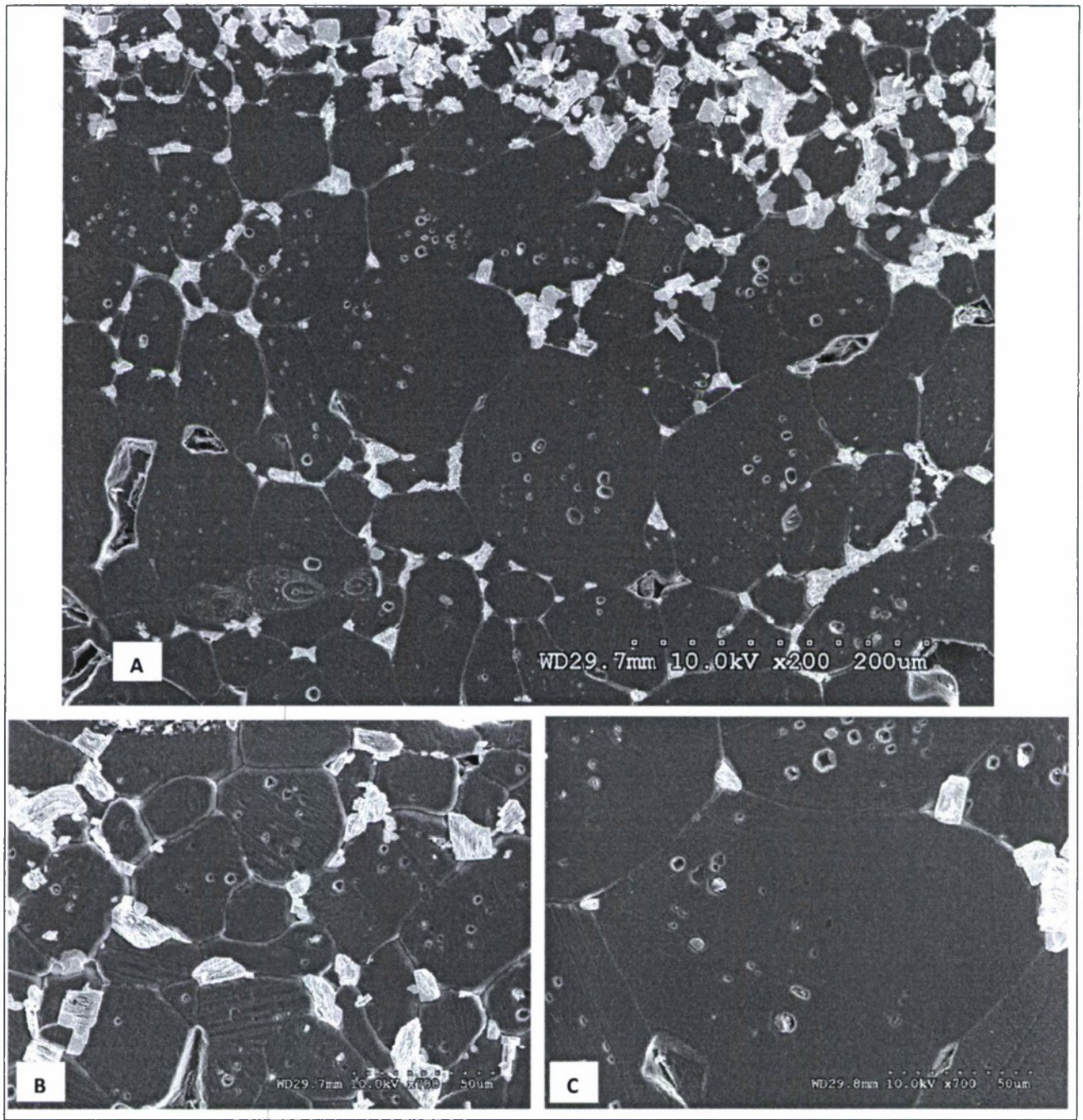


**Figure 6. SEM images of yttria boron carbide sandwich samples heat treated at 1900°C for 15 hours; (A) general overview of the sample, (B) Area very close to the interface, (C) Area away from the interface.**

The microstructure of the yttria-boron carbide sandwich samples were investigated with the aid of SEM and TEM. Figure 6 shows a SEM image of the sandwich sample taken at low magnification as well images of areas at different distance from the yttria/boron carbide mixture and boron carbide interface. Figure 6(A) shows a general overview of the sample. The top edge of the image is the interface between the boron carbide and the yttria/boron carbide mixture. The top of the micrograph is closer to the

interface. Near the interface, yttria particles can be observed intermixed with boron carbide. Further from the interface the yttria is present in the pockets at the triple junctions and also along grain boundaries as discontinuous beads similar to those observed in 1 wt% yttria doped samples. The average grain size of boron carbide is plotted as a function of the distance from the yttria/boron carbide mixture layer in Figure 7. The grain size variation is symmetrical on each side of the sandwich structure. The results can be directly correlated to the concentration of yttria in boron carbide. Closer to the interface the boron carbide grains are heavily pinned by the large volume fraction of yttria. As a result, the average grain size was relatively smaller in that region. The pinning effect becomes progressively negligible further away from the interface. The grain size reaches a maximum (~ 240 μm) at a distance of about 1 mm from the interface. *This strongly indicates activation of a high mobility high order complexion over that concentration range.* As the distance from the interface increases further, the grain size decreases. At a distance of ~3 mm the grain size is about 50 μm; same as observed for 1 wt. % yttria doped boron carbide.

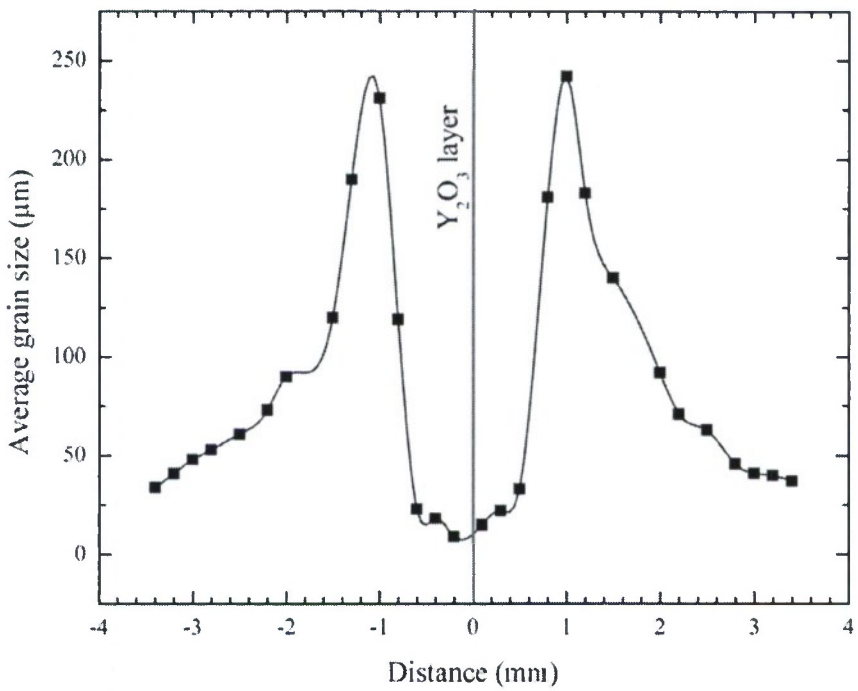


**Figure 7. Grain Size distribution of boron carbide in the sandwich sample. The peak in grain size is a strong indicator a grain boundary complexion change in the system.**

Figure 8 shows a yttria impregnated grain boundary in the sample. It appears that the yttria is present as a discontinuous film on the boundary. This is quite distinct from the continuous IGF so commonly observed in silicon nitride based ceramics. Figure 9 shows a TEM images confirming a discontinuous distribution of the yttria. At this stage it is difficult to determine if the discontinuity is genuine or results from dewetting upon cooling.

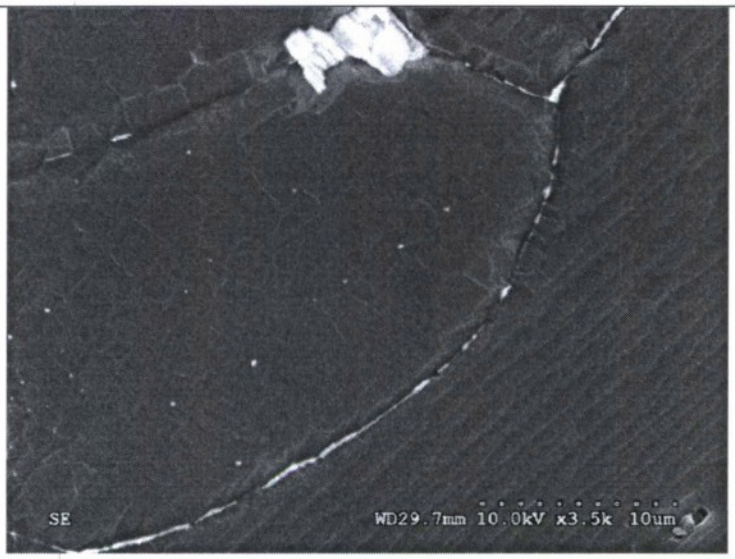


Figure 8. Secondary electron image of a grain boundary in the sandwich sample.

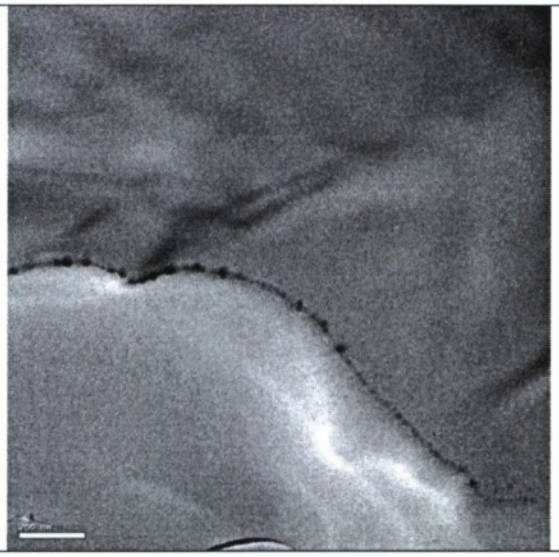

Figure 9. TEM images of an intergranular film in the sandwich sample.

However, the tendency of the film to form beads indicates a dewetting behavior. The weak interface between the yttria and the boron carbide conform to the dewetting behavior. There is a possibility of a complexion transition as the sample is cooled down in the furnace. At high temperature the intergranular film may be a wetting film. As the sample is cooled down there is a complexion transition and dewetting film is formed and the material tries to form clusters and recede to the triple junctions. A faster cooling (preferably quenching) would allow us to preserve the wetting films at the boundaries if this is the case. Conversely, holding at a temperature slightly below the transition temperature will allow the entire intergranular film to recede to the triple junction.

Further research is required to confirm this hypothesis. A new furnace setup would be required that will allow quenching of samples at high temperatures. Also the chemistry of the film needs to be investigated. From the scanning microscopy results the films appear to be predominantly yttria. High resolution EELS spectra can reveal more information about the chemistry of the film.

**PPG#161 R3 (Al 0.5%)**

The crystal structure of the powder was determined to be rhombohedral (Space group: R-3m [166]) by x-ray diffraction. All the peaks observed in the x-ray diffraction plot were assigned to boron carbide except for two peaks at 2q = 34.9° and 44.9° (figure 10). The peaks could not be assigned to any known phase. Figure 11A shows a typical SEM image of the sample. No secondary phase was observed in the sample. The average grain size of the sample was ~20 μm. Cracks were observed at certain areas but not extended completely into the matrix (Figure 11B). TEM analysis revealed extensive twinning along the <110> direction in the samples (Figure 12A). Figure 12B shows a typical high resolution TEM image of a grain boundary of an abnormally large grain. *The boundary is dry without any intergranular film leading us to infer that the abnormal grain boundary is of complexion type III, and that Al is responsible for activating a complexion transition from I to III which is responsible for the abnormal growth behavior.* In fact, no intergranular film was observed in any of the boundaries that were investigated in the microscope. Any isolated aluminum oxide pockets were not observed in the microstructure. The aluminum atoms might be absorbed in the lattice. A sub-monolayer of aluminum atoms along the grain boundary is another possibility. It would require ultra high resolution transmission electron microscopy and analytical measurements (EELS) to confirm the location of the aluminum atoms. In certain areas nanofaceting of the grain boundaries was observed (Figure 12C). The orientation of the faceted boundaries needs to be investigated.

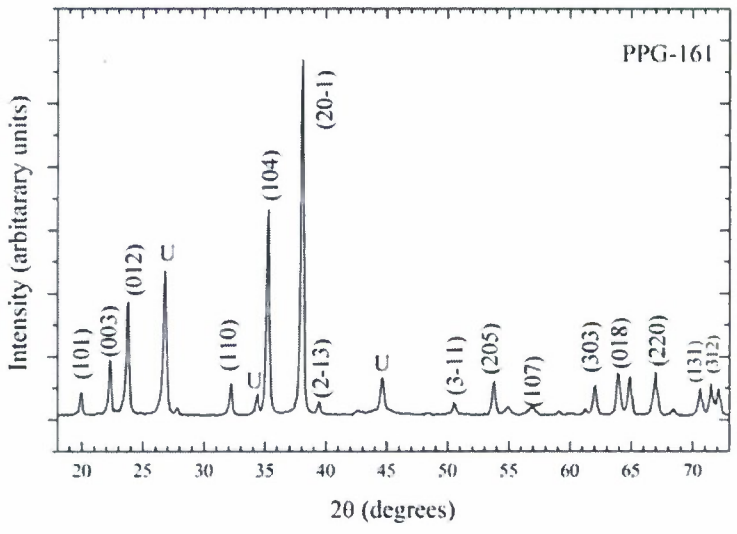


Figure 10. X-ray diffraction Pattern of PPG 161.

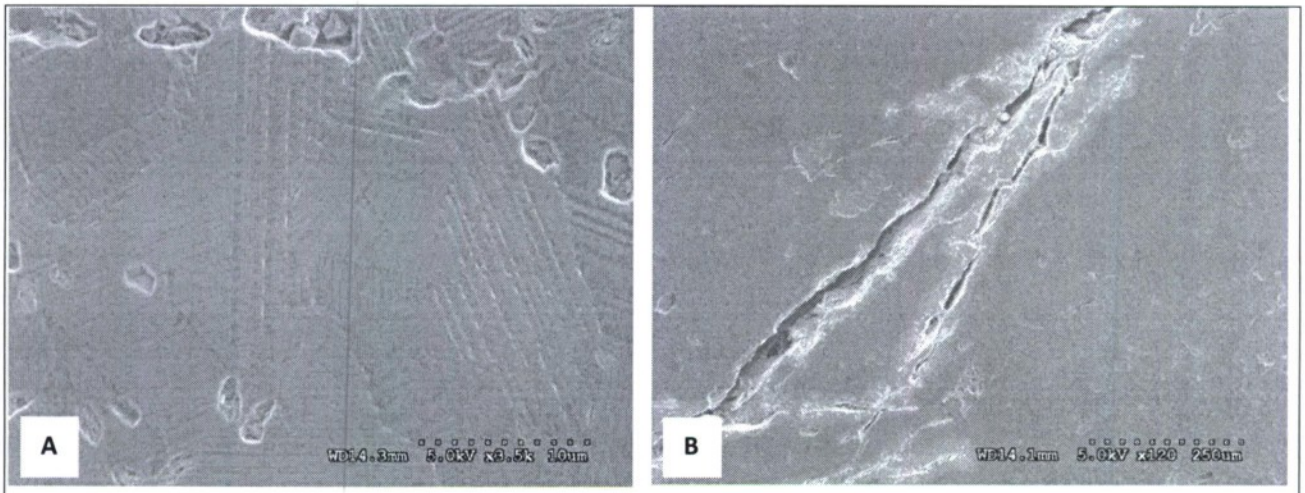


Figure 11. SEM images of PPG#161 sample; (A) typical microstructure, (B) Cracks growing along the grain boundaries.

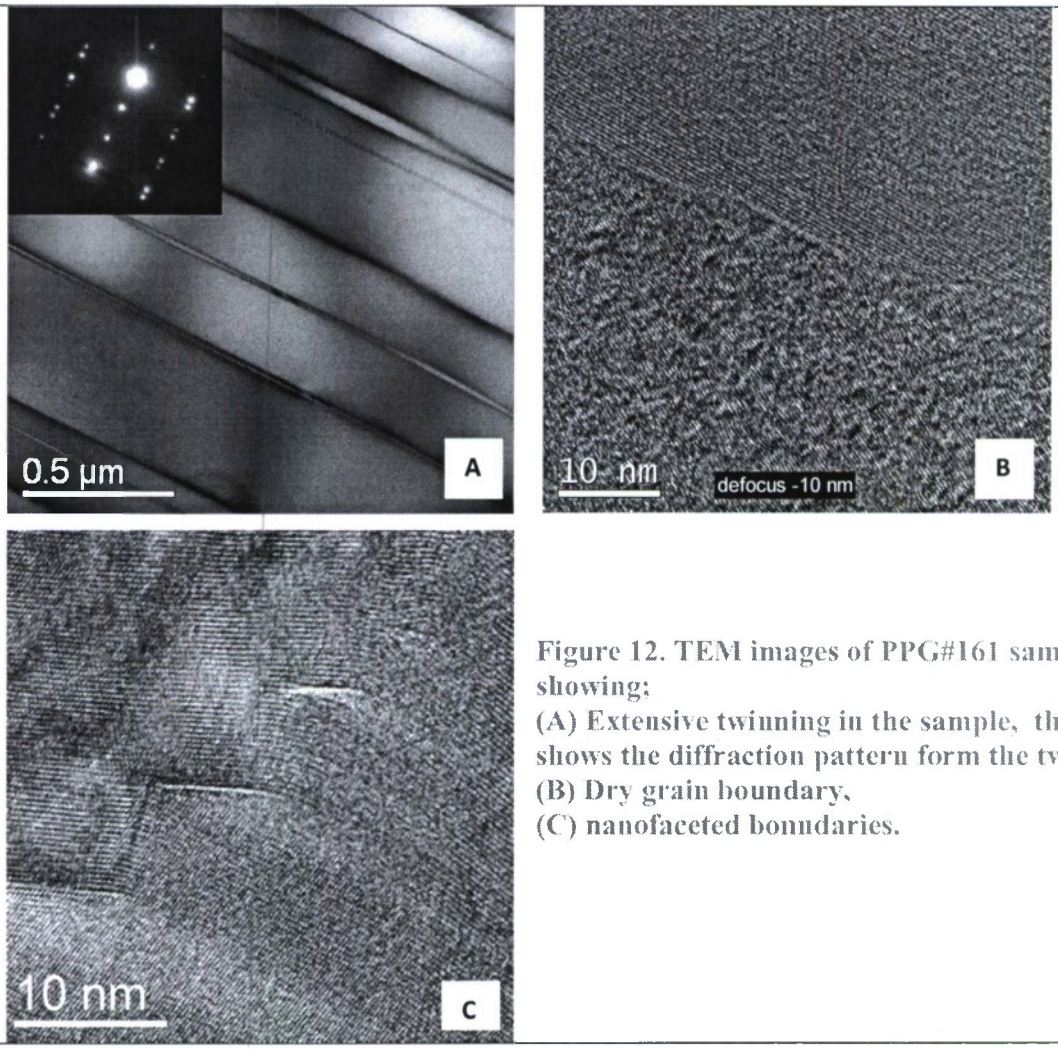


Figure 12. TEM images of PPG#161 sample showing;
(A) Extensive twinning in the sample, the inset shows the diffraction pattern form the twin
(B) Dry grain boundary,
(C) nanofaceted boundaries.

**PPG 166 (Multi dopant, Al, Mg, Si, ---)**

Figure 13A shows a typical microstructure of the sample. The average grain size is about ~8 μm as compared to 20 μm for the alumina doped boron carbide sample (PPG#161) supplied by PPG. Also the multi-dopant sample was less dense as compared to PPG#161. Large cracks similar to those seen in the alumina doped boron carbide supplied by PPG industries were also observed in this sample (Figure 13B). In some instances cracks extended from the large grain into the fine grain matrix. The origin of the stresses could be attributed to their thermal expansion anisotropy. Similar to the previous sample, TEM studies revealed that [110] twins were prevalent throughout the sample. A typical example is shown in Figure 14. From the diffraction pattern it was determined that the boron carbide phase in the sample wass rhombohedral.

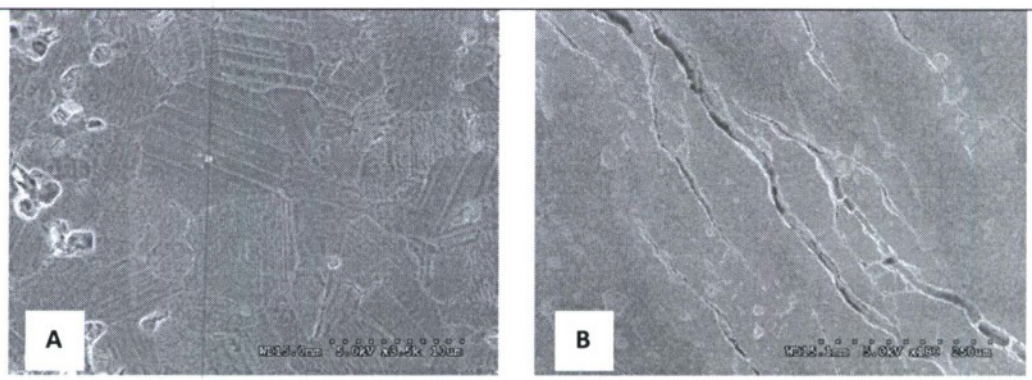


Figure 13. SEM images of PPG#166 sample; (A) typical microstructure, (B) Cracks growing along the grain boundaries.

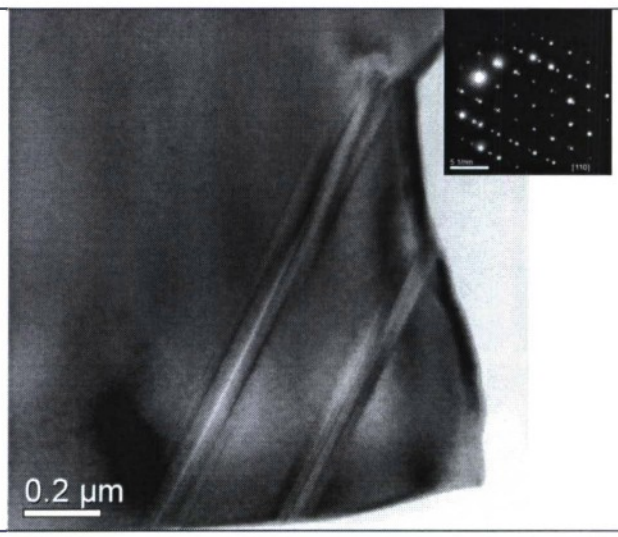


Figure 14.TEM images of PPG#166 sample exhibiting extensive twinning; the inset shows the diffraction pattern from the sample indicating it to be a [110] twin.

Since the processing history and the properties of the starting materials of the PPG samples are not known to us at this time, it is difficult to compare the results with certainty. Assuming that both the PPG

samples were prepared from the same starting materials (identical grain size and particle size distribution), it can be inferred that the presence of the multiple dopants hindered the grain growth in boron carbide by stabilizing a type 1 complexion. Also the grain boundaries were dry for both the samples indicating a grain boundary complexion either of the first three types in the classification. A perfectly clean boundary (Type II complexions) is almost never present in real samples. Hence the grain boundary has either a sub-monolayer segregation (type I) or bilayer segregation (Type III) of dopants at its core. Further investigation is required to ascertain the boundary complexion.

## Conclusions

The main conclusions that can be drawn from the current work are as follows:

1. Sintering and grain growth in boron carbide is highly sensitive to dopant chemistry and amount.
2. A novel processing strategy employing the use of a chemical gradient was effective in revealing the activation of complexion transitions in yttria-doped boron carbide.
3. Alumina promotes abnormal grain growth in boron carbide by activating a grain boundary complexion transition from type I (sub monolayer adsorption) to type III (multilayer adsorption)
4. The use of multiple dopants is effective in stabilizing grain boundary complexion type I in boron carbide and in preventing abnormal grain growth.
5. Further work on the identification and control of grain boundary complexions in boron carbide is highly recommended.

## References


1. Zhang, X.F. and R. Wang, *Short-range order in nanoscale amorphous intergranular films in liquid-phase sintered silicon carbide.* Applied Physics Letters, 2006. **89**(21): p. 211902/1-211902/3.
2. Volz, E., et al., *Formation of intergranular amorphous films during the microstructural development of liquid phase sintered silicon carbide ceramics.* Journal of Materials Science, 2004. **39**(13): p. 4095-4101.
3. Doeblinger, M., et al., *Intergranular films in $Si_3N_4$ studied by TEM.* Institute of Physics Conference Series, 2004. **179**(Electron Microscopy and Analysis 2003): p. 401-404.
4. Becher, P.F., et al., *The importance of amorphous intergranular films in self-reinforced Si3N4 ceramics.* Acta Materialia, 2000. **48**(18/19): p. 4493-4499.
5. Tanaka, I., et al., *Compositions and thicknesses of grain boundary films in Ca-doped silicon nitride ceramics.* NATO ASI Series, Series E: Applied Sciences, 1994. **276**: p. 275-89.
6. Gu, H., R.M. Cannon, and M. Ruhle, *Composition and chemical width of ultrathin amorphous films at grain boundaries in silicon nitride.* Journal of Materials Research, 1998. **13**(2): p. 376-387.
7. Dwyer, C., et al., *Interfacial structure in silicon nitride sintered with lanthanide oxide.* Journal of Materials Science, 2006. **41**(14): p. 4405-4412.

8. Shibata, N., et al., *Observation of rare-earth segregation in silicon nitride ceramics at subnanometer dimensions.* Nature (London, United Kingdom), 2004. **428**(6984): p. 730- 733.
9. Duval-Riviere, M.L. and J. Vicens, *Intergranular film analyses in a-SiC sintered with Al-additives.* Journal de Physique IV: Proceedings, 1993. **3**(C7, 3RD EUROPEAN CONFERENCE ON ADVANCED MATERIALS AND PROCESSES, 1993, VOL. 2): p. 1417-20.
10. Falk, L.K.L., *Imaging and microanalysis of liquid phase sintered silicon-based ceramic microstructures.* Journal of Materials Science, 2004. **39**(22): p. 6655-6673.
11. Falk, L.K.L., *Microstructure development during liquid phase sintering of silicon carbide ceramics.* Journal of the European Ceramic Society, 1997. **17**(8): p. 983-994.
12. Falk, L.K.L., *Intergranular microstructure of liquid phase sintered SiC ceramics.* Advances in Science and Technology (Faenza, Italy), 1995. **3C**(Ceramics: Charting the Future): p. 1925-1932.
13. Hamminger, R., G. Grathwohl, and F. Thuemmler, *Microanalytical investigation of sintered silicon carbide. Part 2. Study of the grain boundaries of sintered SiC by high resolution Auger electron spectroscopy.* Journal of Materials Science, 1983. **18**(10): p. 3154-60.
14. Hannink, R.H.J., et al., *Microstructural investigation and indentation response of pressureless-sintered a- and b-silicon carbide.* Journal of Materials Science, 1988. **23**(6): p. 2093-101.
15. Kim, Y.-W., et al., *High-temperature strength of liquid-phase-sintered SiC ceramics with oxynitride glass.* Key Engineering Materials, 2003. **247**(Advanced Ceramics and Composites): p. 267-270.
16. Liu, M. and S. Nemat-Nasser, *The microstructure and boundary phases of in-situ reinforced silicon nitride.* Materials Science & Engineering, A: Structural Materials: Properties, Microstructure and Processing, 1998. **A254**(1-2): p. 242-252.
17. Turan, S. and K.M. Knowles, *A comparison of the microstructure of silicon nitridesilicon carbide composites made with and without deoxidized starting material.* Journal of Microscopy (Oxford, United Kingdom), 1995. **177**(3): p. 287-304.
18. Ching, W.Y., et al., *Ab initio modeling of clean and Y-doped grain boundaries in alumina and intergranular glassy films (IGF) in b-$Si_3N_4$.* Journal of Materials Science, 2006. **41**(16): p. 5061-5067.
19. Gu, H., et al., *Structure and chemistry of intergranular films in Ca-doped $Si_3N_4$.* Materials Science Forum, 1996. **207-209**(Pt. 2, Intergranular and Interphase Boundaries in Materials): p. 729-732.
20. Nishimura, H., et al., *Internal friction analysis of CaO-doped silicon carbides.* Materials Transactions, 2002. **43**(7): p. 1552-1556.
21. Siegelin, F., H.J. Kleebe, and L.S. Sigl, *Interface characteristics affecting electrical properties of Y-doped SiC.* Journal of Materials Research, 2003. **18**(11): p. 2608-2617.
22. Tanaka, I., et al., *Calcium concentration dependence of the intergranular film thickness in silicon nitride.* Journal of the American Ceramic Society, 1994. **77**(4): p. 911-14.
23. Doen, B. and P. Gadaud, *Silicon nitride and YMgSiAlON glass study by mechanical spectroscopy.* Journal de Physique IV, 1996. **6**(C8, ICIFUAS 11, Eleventh International Conference on Internal Friction and Ultrasonic Attenuation in Solids, 1996): p. 707-710.
24. Choi, H.-J., J.-G. Lee, and Y.-W. Kim, *Oxidation behavior of liquid-phase sintered silicon carbide with aluminum nitride and rare-earth oxides ($Re_2O_3$, where Re = Y, Er,Yb).* Journal of the American Ceramic Society, 2002. **85**(9): p. 2281-2286.
25. Cinibulk, M.K., et al., *Amorphous intergranular films in silicon nitride ceramics quenched from high temperatures.* Journal of the American Ceramic Society, 1993. **76**(11): p. 2801-8.
26. Dillon, S.J., Tang, M., Carter, W.C., and M.P. Harmer, *Complexion: A New Concept for Kinetic Engineering in Materials Science.* Acta Materialia, 2007. **55**: p. 6208-18.

27. Dillon, S.J. and M.P. Harmer, *Multiple Grain boundary transitions in Ceramics: A Case Study of Alumina.* Acta Materialia, 2007. **55**: p. 5247-54.
28. Dillon, S. J., *Relationship between Grain Boundary Complexion and Grain Growth Kinetics in Alumina.* PhD Dissertation, Lehigh University, 2007.
29. Weaver, G.Q., *Sintered High Density Boron Carbide*. US Patent 4,320,204.
30. Lee, C.H. and C. H. Kim, *Presureless Sintering and Related Reaction Phenomena of $Al_2O_3$-doped $B_4C$*. Journal of Materials Science, 1992. **27**: p. 6335-40.
31. Skorokho, V. Jr., Vlajic, M.D., and V.D. Krstic, *Mechanical Properties of Presureless Sintered Boron Carbide Containing $TiB_2$ Phase*. Journal of Materials Science Letters, 1996. **15**: p. 1337-39.
32. Kanno, Y., Kawase, K., and K. Nakano, *Additive Effect on Sintering of Boron Carbide. Journal of ceramic Society of Japan*, 1987. **95**: p. 1137-40.
33. Zakhariev. Z., and D. Radev, *Properties of Polycrystalline Boron Carbide Sintered in the Presence of $W_2B_5$ without Pressing*. Journal of Materials Science Letters, 1988. 7: p. 695-96.
34. http://www.hcstarck.de/medien/dokumente/document_4_acp_13_web.pdf.